Investigation of Mechanical Behaviors of Motorcycle Frames Designed from Steel and Hybrid Materials under Static and Dynamic Loading

Serkan TABAK[1] [ID], Recep EKICI[2, *] [ID]

[1] *Graduate School of Natural and Applied Sciences, Erciyes University, Kayseri 38039, Türkiye*
[2] *Department of Mechanical Engineering, Erciyes University, Kayseri 38039, Türkiye*

Highlights
• Strength analyses of a chopper type motorcycle frame under static and dynamic loads were performed.
• Strength analyses were carried out using the Finite Elements Method.
• The stress and safety coefficient values of the hybrid frame were higher.
• The total deformation values of the steel frame are lower.
• The strength values of the steel frame are better than the hybrid frame.

Abstract

Motorcycle use is increasing and becoming widespread every day in the world, especially in Turkey. As the need for motorcycles increases, the basic structural parts of motorcycles, especially the frames, are desired to be stronger and cheaper as well as lighter. For this reason, although motorcycle frame materials are mostly steel or aluminum, in recent years hybrid materials consisting of composites and various alloys, especially in frame construction, have become widespread in the motorcycle industry. In this study, a preliminary design of two separate motorcycle frames consisting of steel and hybrid (steel, aluminum alloy and carbon fiber reinforced polymer (CFRP) composites) materials were made with solid modeling, and a finite element model of both frames was created. Thus, the deformations and stresses created by the static and dynamic loads acting on the frame were analyzed, and the frames were compared in terms of static and acceleration loading.

1. INTRODUCTION

The loads acting on the motorcycle frame during its lifetime are mainly; static weights of the driver and passenger, engine-transmission and other accessories, dynamic loads arising from the road, and acceleration-deceleration inertia. A motorcycle frame exposed to such static and dynamic load conditions should not deform excessively, have optimum strength and rigidity to carry all loads, and should maintain the structural stability of the vehicle. In addition to these enhanced strength properties, the availability of materials and ease of production are important factors, which affect the production cost of a motorcycle. However, nowadays, lightness is one of the most important factors desired due to fuel efficiency for customers. Also, it is desired that it requires little maintenance during use after production and is not affected too much by environmental conditions.

The construction of a steel motorcycle frame takes a long time and requires expert Mig/Tig welding. On the other hand, as a result of long-term use, corrosion in the weld seams, defects in the weld seam and fatigue due to faults, cracks, and breaks may occur. In order to minimize these disadvantages, frames made of composites such as CFRP, which attract attention with their strength and lightness, have come to the fore recently. It is expected that a solid tube joint can be obtained by cutting CFRP tubes in appropriate sizes, processing the ends of metal materials (like the neck stem of the frame) in the appropriate form, gluing them with epoxy resin, applying carbon and/or kevlar fabrics (prepreg) to support the frame joints. Thus, a

*Corresponding author, e-mail: rekici@erciyes.edu.tr

frame can be produced in a faster time than welded manufacturing, does not require expert welding labor, shows more strength, and is resistant to cracks and breaks can be made. Also, with the motorcycle frame to be created using CFRP composites, a lighter frame will be obtained compared to the steel frame. In this way, it is estimated that the lifetime of the motorcycle will be longer with the use of a composite frame that is resistant to corrosion and vibration and has natural damping properties. On the other hand, it is thought that fuel consumption will decrease due to the composite frame, which is lighter in weight than the steel frame. In addition to this, Mateusz *et al.* [1] compared several possible chassis configurations, including the design with several areas reinforced using CFRP and with the additional stiffening element mounted. They observed that the use of CFRP reinforced sections increases the life of a chassis due to the orthotropic structure of CFRP. Also, Fentahun and Savaş [2] stated that CFRPs provide some advantages, such as the potential for maximum mass reduction in vehicles and the potential to reduce carbon emissions by making the vehicle lighter.

In the literature and production sector research conducted within the scope of this study, a Chopper-style motorcycle frame made of carbon fiber material and tubing has never been encountered. However, similar studies found in the literature are given here. In the study of Jeyapandiarajan *et al.*, [3] attempts were made to design a structurally stable chassis for an electric motorcycle. Thus, real-time forces on the chassis were simulated with 3 different materials, AISI 1020, Aluminum 6063-T6 and AISI 4340, considering various parameters obtained from the literature research. It has been tried to determine the most suitable material for the targeted chassis. Dama *et al.* [4] produced an automotive Flex Body Space-Frame Structured prototype using the finite element modeling and analysis method. This prototype work was produced with Additive Manufacturing technology using Fused Deposition Modeling Technique in a shorter time and at lower cost. Mat and Ghani [5] designed a lightweight and low frictional resistance chassis for "Eco-Challenge" race cars in their study in 2012, and examined the behavior of this chassis when subjected to normal vehicle loads such as engine and driver weight, acceleration, braking and cornering forces. This chassis should also have been able to protect the driver in the event of a collision. A steel space frame was chosen for the chassis design in question. The chassis is simulated with five different loading conditions. These were the static load (dead load) of the vehicle supported on the axle base was 4g load on the main pulley, 1.5g acceleration, 1.5g deceleration (braking) and 2500 Nm/degree torsional load.

A structural analysis of a motorcycle planned to be produced by the Ajp brand was carried out by Rechena [6] using the finite element method. With static simulations and bending analysis for parts under compression loads, the loads and safety factors that will act on the vehicle were tried to be estimated. In another study by Liang *et al.* [7] in 2014, the fatigue life of a motorcycle frame made of two different materials was estimated by conducting a road trial together with computational simulation studies based on the finite element analysis method. In the study by Tripathi and Ambikesh [8], carbon-flax hybrid composite was used instead of steel for the motorcycle frame. With this new material combination, FEM analysis of the motorcycle frame was performed for various loads under static conditions. It was observed that the maximum deformation occurred in the driver tube and it was stated that this could be improved in terms of strength by providing an extra rod support from below.

In the study conducted by Neeraja *et al.* in 2012, a frame was modeled using 3D modeling software Pro / Engineer, a structural analysis was made by applying wheel forces to verify the strength of the frame, and the final stress limit for the model was determined in this analysis. Four materials (alloy steel, aluminum alloy A360, magnesium and CFRP) were studied to select the best material for the frame. In the results of working; It has been determined that the stress values for all materials are lower than the allowable yield stress values, so that the design is safe. Comparing the results for the four materials, the stress is the same and the displacement is less for the CFRP material than for the other three materials. Therefore, for the design, it was concluded that CFRP is a more suitable material for the suspension frame. In addition, for future work; It has been stated that the model can be prepared properly by using CFRP composite, this material is the most suitable material for the production process since it has less density compared to other materials used in frame production, it can withstand very high loads and reduces the cost of frame manufacturing. It has been emphasized that CFRP has an almost infinite service life when protected from the sun, and unlike steel alloys, there is no durability limit when subjected to cyclic loading [9]. In the thesis of Slaiman in 2018, it was stated that CFRP material gives good strength and a lighter weight compared to

steel and aluminum, while carbon fiber like titanium is also very expensive. It has been emphasized that motorcycle frames produced with CFRP are good in theory, but cannot be used as long as frames made from other materials. Thus, it has been argued that only a few bicycle frames were produced with CFRP, carbon was combined with epoxy to achieve good results, but could never be used in motorcycle frames [10].

In addition, when the production sector is examined, it has been seen that carbon fiber has been tried in the construction of the frame of some motorcycles. In particular, BMW company has made some trials for the production of motorcycles with carbon fiber frame [11], but these studies could not pass to the mass production stage. In 1983, Honda company produced a futuristic Nr500 model motorcycle with a full carbon fiber frame. This production has never competed in official races, but has been a test run for the future.

Many small manufacturing companies have experimented with carbon fiber frame. In 1990, businessman Piero Ferrari created a spectacular carbon fiber frame for Cagiva's 500 Gp motorcycle. Famous motorcycle racer Randy Mamola has tested the frame, which is very accurately steered but produces a lot of vibration. It has been observed that this frame produced is quite rigid [12]. In 1985, the Honda Cbx750 Black Buffalo model motorcycle with a carbon fiber frame was produced by the Japanese racing car manufacturer Dome. The driver of the motorcycle said; "Black Buffalo worked very well and remained intact when I crashed at high speed. To me, it seems inevitable that this technology will feed Moto Gp." However, not a single carbon fiber frame motorcycle was produced that competed in the motorcycle racing industry until 2019.

Garofano *et al.* in the study of [13] in 2023, they investigated the use of laminated composite panels in an electric minibus chassis as an effective way to reduce the global mass of the chassis structure and at the same time increase their structural performance in terms of torsional stiffness and crashworthiness. By replacing specific steel tubes with CFRP laminated composite structures, different chassis configurations were numerically developed and detailed simulations were performed to compare both masses and mechanical responses.

In this study, a preliminary design of a motorcycle frame has been made, which has not been done before. Static and dynamic loading analyzes were carried out for two separate motorcycle frames made of only steel and hybrid use of CFRP composites with aluminum and steel materials using the finite element method. As a result, the strength behavior of the pre-designed motorcycle frame was revealed. Thus, it was aimed to create a lightweight and robust hybrid frame structure that can be used in motorcycles. In this study, mechanical vibrations originating from the engine/road and fatigue strength were not considered. In the study, the torsional loads on the frame designed from the tube were not taken into account. Only the tensile and compressive stresses in the pipes are taken into account. In addition, the behavior of the motorcycle chassis design in case of impact has not been examined. The impact phenomenon and fatigue will be examined in the future as another study subject.

2. MATERIAL METHOD

2.1. Preliminary Design with Solid Modeling and Material Properties

In the study, the motorcycle frame whose geometry is designed as tubular is the frame of a "chopper" model motorcycle. The main reason for choosing the chopper model motorcycle is that this type of motorcycle is a simple and durable vehicle with the least possible equipment. In the preliminary design, the connection interfaces of the engine-transmission and other sub-equipment were not included, only the frame was designed. As a result of the structural strength analyses, it was planned to complete the missing connection interfaces on the frame at the final design and prototype stage. This study includes only structural strength analysis and does not include fatigue analysis, final design, and prototype production stages.

Solid modeling of the motorcycle frame was done in Solidworks software. Two different frames were modeled in order to determine the advantages and disadvantages by comparing them with each other; the first of these is designed from steel material with welded manufacturing, and the second is a hybrid frame

made of CFRP, aluminum and steel materials. A simple motorcycle design made is given in Figure 1. Only the frame type changes in the designs, and the other systems are exactly the same.
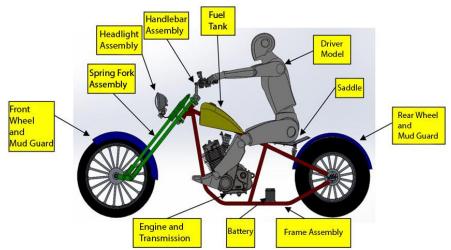

Figure 1. *Motorcycle preliminary design model*

This model was used in static and dynamic loading analysis. The Solid model; includes the frame, fuel tank, engine-transmission, front fork, front fender, rear fender, front wheel and rim, rear wheel and rim, seat, front light, handlebar, battery, other small parts (front and rear axles), and driver. The remaining other components (wiring, hydraulic tube connections, alternator, starter, etc.) were added to the final design, their weight was included in the frame weight and considered in the analyses.

The most characteristic features of a motorcycle are the steering axis, the rake angle, the front ground trail, the rear ground tail and the center of gravity [14]. These characteristic features were determined in appropriate value ranges and applied to the frame.

Within the scope of detailed preliminary design studies; Modeling of wheels and rims has been done. International standards were used in these solid modeling studies; Iso 5751-1 (Motorcycle Tires and Rims-Part 1: Design Guides) [15], Iso 5751-2 (Motorcycle Tires and Rims (Metric Series)-Tyre Sizes and Load Carrying Capacities) [16] and Iso 4249-3 (Motorcycle tires and rims- Part 3: Rims) [17]. At the end of the study; 160/80B16 rear wheel size and 90/90-21 front wheel size were determined, wheel and rim sections, and solid models were created according to the aforementioned standards. On the other hand, the "Old School Chopper Frame Fabrication" descriptions given in The Chopper Builders Handbook [18] were used in modeling the tube assembly of the frame.

After solid modeling, ANSYS Finite Element Analysis (FEA) software [19] was used for static and dynamic analyses. For this purpose, solid models of designed motorcycle frames were imported to ANSYS FEA software to apply finite element method procedures (defining connections, material properties, Mesh, etc.). Other modeling details of each frame was given below.

2.2. Modeling Details of the Steel Frame

The image of the frame made of Aisi 4130 (St 37-2) steel material is given in Figure 2. It is envisaged that the joints of all parts of this frame are welded, and all welded seams are considered to be flawless.
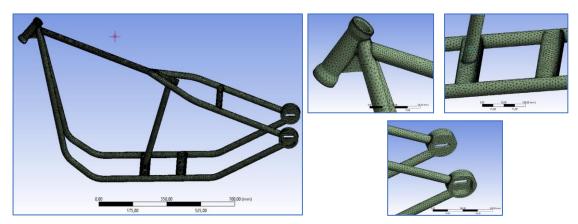
Figure 2. *Frame design with steel material and mesh structure*

The mesh structure of the designed steel frame was created and it is confirmed that it is suitable for the meshing quality criteria of Element Quality, Aspect Ratio, Skewness, Jacobian Ratio and Orthogonal Quality of the ANSYS FEA software. Accordingly, the steel frame consists of 426.272 nodes and 255.475 elements. Tet10 (10 nodes tetrahedral) elements were used in steel chassis meshing.

2.3. Modeling Details of the Hybrid Frame

There are three different materials in the structure of the hybrid frame. In fact, it was originally planned to be designed with two materials (aluminum alloy and CFRP composites). However, it was decided to use AISI 4130 material for the parts to be bent, since the aluminum material causes problems by cracking during the bending process. For the four difficult parts that require angled joints; it has been decided to manufacture them with the additive manufacturing method in order to be easy to manufacture and to add an originality to this work. Additive manufacturing was carried out by Fatih Sultan Mehmet University Aluteam Laboratory in Istanbul. The image of the frame designed with the hybrid use of AISI 4130, CFRP composites, and AlSi10Mg materials is given in Figure 3.
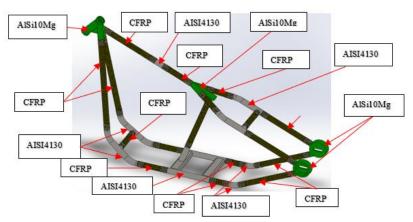

Figure 3. *Frame design with hybrid materials*

It is assumed that the Aluminum, steel and CFRP composite parts in the Hybrid Frame were bonded together with 0.5 mm thick epoxy adhesive used in the aerospace industry. In the connections, epoxy adhesive and other parts (aluminum and steel) were assumed to join perfectly. CFRP composite tubes have outer diameter of 32 mm. In addition, the wall thickness of CFRP composite tubes was assumed as 1.5 mm, namely, CFRP composite tubes were modeled from 5-layer carbon fibers (each layer is 0.3 mm thickness) with 0°/90° fiber stacking configuration. Besides, all parts in the FEA model were assumed to have linear elastic properties. The physical properties of the materials used in the study are given in Table 1.

***Table 1.** Material properties (from Ansys Material Library)*

Property	CFRP	AISI4130 (Normalized)	AlSi10Mg	Epoxy Resin
Density [gr/cm^3]	1.42	7.83	2.67	1.16
Poisson Ratio	0.30	0.32	0.33	0.35
Modulus of Elasticity 0° [GPa]	61.3	206.1	72.0	3.78
Modulus of Elasticity 90° [GPa]	61.3	206.1	72.0	3.78
Yield Strength 0° [MPa]	805.0	507.8	251.0	54.6
Yield Strenght 90° [MPa]	805.0	507.8	251.0	54.6

Since the hybrid frame does not consist of a single material as in the steel frame, some preparations were made before the analysis. First of all, since the hybrid frame consists of two metals, composite materials, and epoxy adhesives, a frame analysis model consisting of different materials had to be created. For this process, the "Mechanical Model" and "Acp (Pre)" sub-modules must be created on the Ansys Workbench platform. Before analysis, solid models of all different materials are prepared for analysis in separate sub-modules. These solid models will then be combined in the same space environment for analysis.

The solid analysis model, which we have simplified by removing the holes in the Space Claim and Design Modeler modules in Ansys, is created only for 12 isotropic metal parts (AlSi10Mg and AISI 4130). In this context, the image of the FEA models of metal parts consisting of 4 AlSi10Mg and 8 AISI 4130 parts in the Ansys Mechanical Model Design Modeler module is given in Figure 4.

The composite structures used in the study were modeled in Ansys Composite PrepPost software module. Ansys Composite PrepPost provides all the necessary functionality for the analysis of layered composite structures [17]. The image of 17 pieces of CFRP composite tubes modeled as layers, containing 5 laminates, in the Ansys Acp Pre module is given in Figure 5.
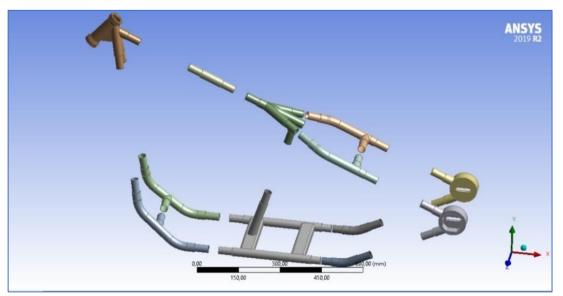

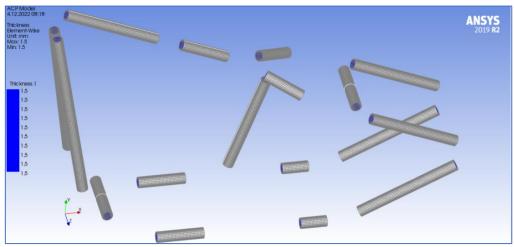***Figure 4.** The view of 12 metal materials in the design modeler module*

Figure 5. *Image of 17 pieces of CFRP tubes in Acp Pre module*

In the hybrid motorcycle frame, all metal- CFRP composite connections were fixed by CFRP composite coating pieces, which were a thickness value of 1.2 mm (formed from 4 layers and assumed each layer was 0.30 mm thick). There are 34 pieces of CFRP Reinforcement Coating parts in the composite material mechanical model (Figure 6).

After the metal and adhesive parts of the hybrid frame are modeled in the "Mechanical Model" and the composite parts in the "Acp (Pre)" module, all solid models were combined in the "Static Structural" analysis environment.

The mesh structure of the solid model created for the hybrid frame is shown in Figure 7. There are 416.182 nodes and 218.428 elements in this structure. The mesh structure has been validated according to the meshing quality criteria of Element Quality, Aspect Ratio, Skewness, Jacobian Ratio (Gauss Points) and Orthogonal Quality of the Ansys program. Tetrahedral, hexahedral, wedge, quad4, quad8 (quadrilateral) and tri3 (triangular) elements were used in hybrid chassis meshing.
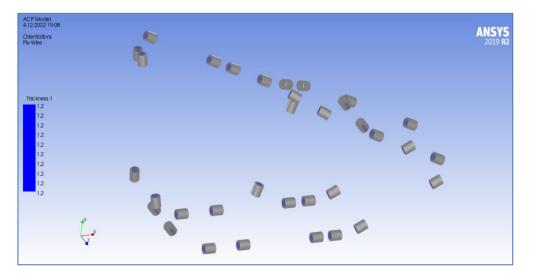

Figure 6. *Image of 34 pieces of CFRP reinforcement coating parts in Acp Pre module*

For example, according to the Jacobian Ratio Gauss Points criterion, the mesh metric average value was found to be 0.931 for the hybrid chassis, and according to the "(Bad) 0-1(Perfect)" criterion, it was determined to be at a very good level.
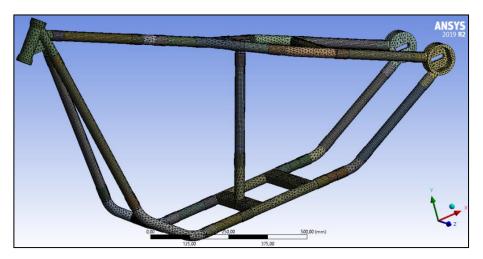
***Figure 7.** Mesh structure of hybrid material frame*

After four solid model groups are combined in the Static Structural module, the process that needs to be done is to arrange the contacts of the "Connections" of the four models to each other. The purpose of this process is to apply bond connections made by metal surfaces with epoxy adhesive, metal surfaces with CFRP tube, epoxy adhesive model with CFRP tube, metal surfaces with coating model, CFRP tube surfaces with coating model. An example of the connection of metal parts with the solid model simulating the bonding zone is given in Figure 8.
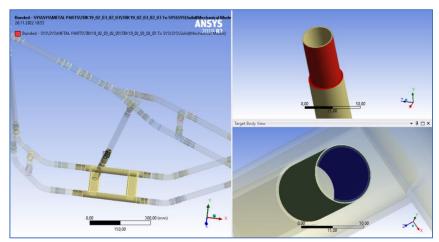

***Figure 8.** Example of bonded metal parts to epoxy adhesive solid model*

As the engine-transmission group is the heaviest component (approximately 25% of the total mass), its position greatly affects the position of the motorcycle's CoG [20].

The load applied on the steel frame designed in this study was designed as a total of 280 kg, with a total motorcycle weight of 180 kg and a driver of 100 kg. 100 kg is too much for the rider, but often riders carry extra load on their bikes, so an additional 20 kg is added to the rider's weight. However, a weight reduction of 10.16 kg has occurred in the hybrid frame due to the use of CFRP composites and aluminum materials.

The CoG of the hybrid frame obtained in the Solidworks program is given in Figure 9. For the CoG measurement, the point where the rear wheel touches the ground is taken as the reference.
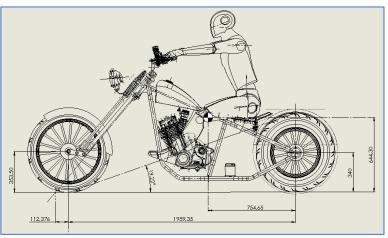
Figure 9. *CoG dimensions of the motorcycle with hybrid frame*

The dimensional and total weight difference between the CoG of motorcycles with steel frame and hybrid frame are given in Table 2. The location of the hybrid frame's own CoG is shown in Figure 10 (a). For static and dynamic loading finite element analyzes, the position of the CoG is changed to the location of the CoG of the main integration. Figure 10 (b) shows the location of the modified CoG.

Table 2. *Motorcycle physical dimensions with steel and hybrid frame*

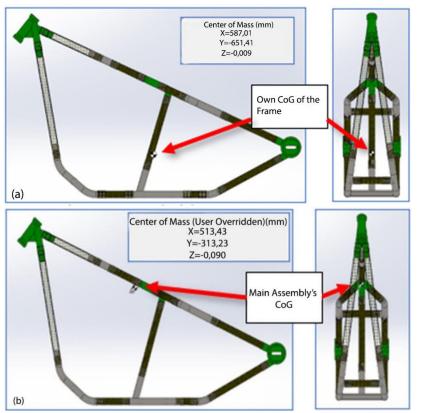| Parameter	CoG to Rear Axle, b[mm]	CoG to Ground, H[mm]	Front and Rear Axle, P[mm]	Trail, B[mm]	Tube Dia., D[mm]	Front Wheel Radius, R_f[mm]	Rear Wheel Radius, R_r[mm]	Motorcycle's Total Mass, m[kg]
Steel frame	749.37	639.20	1959.35	112.37	31.75	353.50	340.0	280.0
Hybrid frame	754.65	644.30	1959.35	112.37	31.75	353.50	340.0	269.8

Figure 10. *a) The location of the hybrid frame's own CoG, b) The location of the modified CoG*

3. FINITE ELEMENT ANALYSIS OF STEEL AND HYBRID FRAMES

3.1. Assumptions for Analyses

Some assumptions used in static and dynamic finite element analyses in the study are given below.

i) The road is considered to be straight (without slope, without water, without snow, asphalt and clean) and in normal condition.

ii) In the calculations, the position change and movements of the rider on the motorcycle while driving will be considered constant. The CoG changes due to this situation will be neglected.

iii) The weight of the fuel and cooling system (water and oil) added to the total mass of the motorcycle equals approximately 13 kg.

iv) Under normal conditions, the position of the CoG will change slightly as the fuel level drops. In this study, the change of the CoG due to fuel reduction is neglected.

v) The load acting on the rear wheel directly acts on the frame. The transfer load during braking and acceleration is considered constant without any loss of energy.

vi) It is assumed that all loads acting on the wheels (rear or front) directly affect the frame of the motorcycle. Therefore, the value of these parameters in the analyses will be much higher than in normal operating conditions, because in this study it is assumed that the shock absorbers do not work. (Although not accepted in this study, some energy will actually be absorbed by the shock absorbers), so the safety factor will be lower than the normal situation, but on the other hand the motorcycle will be controlled in more difficult conditions.

vii) The adhesive joints at the metal part and composite tube joints in the hybrid frame are also modeled as solid. Thus, the behavior of the bonding places whose material is epoxy resin will also be analyzed.

viii) Besides, the designed steel and hybrid frames are modeled as the hard tail.

3.2. Static Load Analysis

The location of the center of gravity and the static forces are shown in Figure 11.
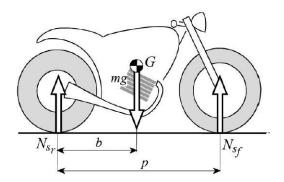

Figure 11. *Position of center of gravity and static forces [18]*

The force exerted by the motorcycle on the ground is given in Equation (1);

$$G = m.g. \tag{1}$$

Here, m is the mass, and g is the gravitational acceleration. The front wheel load of the motorcycle in the static state is given in Equation (2);

$$N_{sf} = \frac{b.G}{p}. \tag{2}$$

The rear wheel load of the motorcycle in the static state is given in Equation (3);

$$N_{sr} = \frac{G.(p-b)}{p} \quad . \tag{3}$$

According to the balance of static forces, the application of the gravity force from the CoG, the application of the N_{sf} and N_{sr} (divided by two, applied from each axle housing) forces on the solid model and the boundary conditions are shown in Figure 12.
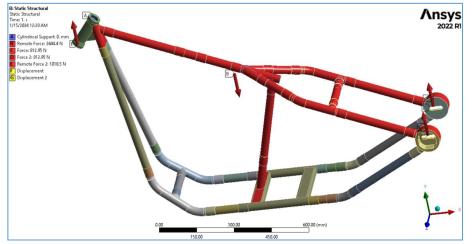

Figure 12. *Application of forces and boundary conditions for static loading analysis*

Here, the motorcycle front wheel load N_{sf} is assumed to act on the steel frame and applied from the steering neck, although some of the forces from the ground are damped due to the presence of shock absorber springs in the front fork. As the boundary conditions; "Cylindrical Support" was applied from the bearings in the steering neck, where the radial and axial movements of the cylindrical support were released and the tangential movement was fixed. A "Displacement Support" was applied from the right and left rear axle housings, where the movement in the x and z axes was fixed, only the movement in the y axis was allowed (When the z axis was fixed and the x and y axes were released, the solution of the finite element method could not be reached, an error occurred in the analysis).

Accordingly, as a result of the static loading analysis made in steel and hybrid frames; Total deformations are given in Figure 13, Equivalent (Von-Misses) Stresses are given in Figure 14.
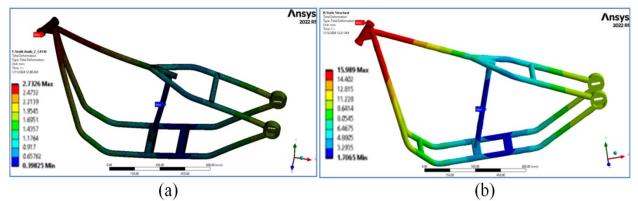

(a)　　　　　　　　　　　　　　　　　(b)

Figure 13. *Total deformation for static analysis (a) Steel Frame (b) Hybrid Frame*
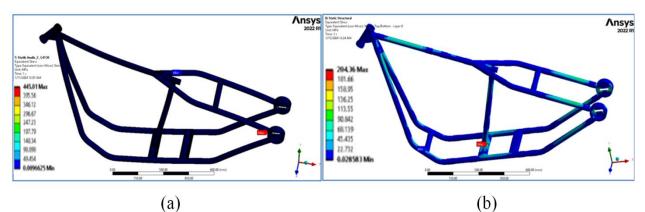
Figure 14. Von-Mises stress for static analysis (a) Steel frame (b) Hybrid frame

After the static loading analysis, the detailed pictures of the regions where the maximum stresses occur in the hybrid frame are shown in Figure 15.
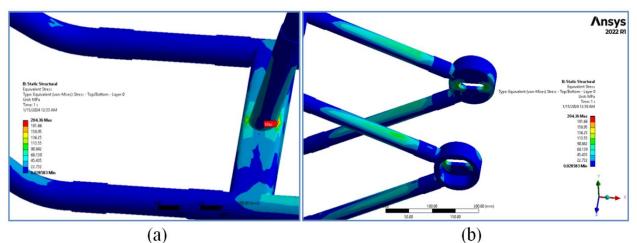

Figure 15. Maximum equivalent (Von-Mises) stress distribution under static loading analysis in (a) AISI 4130 region, and (b)AlSi10Mg region (Detailed Pictures)

Comparison of static loading analyzes of steel and hybrid frames is shown in Table 3. In terms of max. total deformation, it is seen that the deformation value of the hybrid frame is considerably higher than the deformation value of the steel frame. It is considered that this is due to the fact that the steel frame has a more rigid structure due to its welded joint structure, while the hybrid frame is due to the integration of a large number of parts joined by bonded joints. In addition, it is considered that the maximum deformations in the neck of the frame will be much lower under real operating conditions due to the presence of springer fork and front wheel. On the other hand, considering that the engine and transmission group will also be connected to the frame under real operating conditions, it is certain that the deformation values will be much lower.

Table 3. Comparison of steel and hybrid frames

Nm.	Feature/Analysis result	Units	Steel frame	Hybrid frame
1	Max. total deformation	[mm]	2.73	15.98
2	Max. equiv. Von-Mises stress	[MPa]	445.01	204.36
3	Safety coefficient	-	1.1	2.5

As can be seen in Figure 15 (a), maximum stress occurred only on the bottom of the seat tube which is made of AISI 4130 steel. According to the analysis result, it has been determined that the safety coefficient of the hybrid frame is s=2.48, according to the 507.8 MPa safety stress specified in Table 1. In the rear axle

housing of the frame, where high stress is detected, safety conditions are provided since the maximum stress value is lower than 251 MPa, which is the safety stress of AlSi10Mg material. In other parts of the frame containing CFRP material; It is seen that the stress values vary between 0-68.139 MPa values, and in this context, the safety factor for other regions is approximately s=11. The safety factor of the steel frame is s=1,1 as it is shown in Table 3. In the case of static loading, the Hybrid frame presents a stronger structure than the steel frame.

3.3. Maximum Acceleration Load Analysis

This section considers all the forces that can affect the motorcycle's frame when the motorcycle is traveling at maximum acceleration (maximum speed equals 130 km/h). Therefore, first, all known parameters (forces) were found, all other parameters were calculated using some static equations (Newton's Second Law, Equilibrium Law and Dynamic Equation) and then, all these parameters were entered into the computer program (As Solidworks design software, Ansys Workbench were used to detect stresses and displacements). Accurate determination of all stresses and displacements of finite elements is important in order to obtain results as accurately as possible. Figure 16 shows all unknown forces that need to be calculated. This calculation study is based on the calculation method of V. Cossalter's work [21].
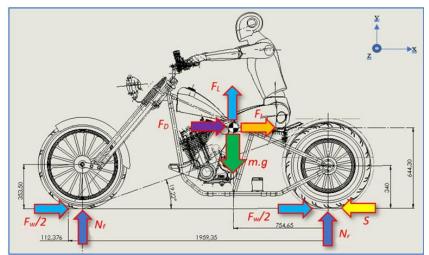

Figure 16. *Forces acting on motorcycle on acceleration for Hybrid Frame*

The forces given in Figure16 are;

- Normal forces N_f and N_r exchanged between road and tires,
- The weight force of the motorcycle acting on the center of gravity, m.g,
- Force of inertia due to acceleration $m.\frac{d^2x}{dt^2}$ (F_I),
- The force S exerted by the ground on the motorcycle at the contact point of the rear wheel in response to the driving force of the motorcycle engine,
- Aerodynamic drag force F_D,
- Tire rolling resistance force F_w,
- The aerodynamic lift force is F_L.

Thus, the drag force acting on the hybrid and steel frames [19];

$$F_D = \frac{1}{2}\rho C_D A V^2 \ . \tag{4}$$

Here ρ is the density of the air, A is the front area of the motorcycle, C_D is the aerodynamic drag coefficient, V is the forward speed of the motorcycle.

$C_DA=0.745$ m^2 value is taken according to [19]. Besides, if the aerodynamic drag coefficient value is compared with the graph in Figure 17 created by Vittore Cossalter [19]; It is seen that for $C_DA=0.74$ m^2 and 130 km/h values, $F_D\sim550$ N will be around, so 566.86 N found by Equation (4) is consistent.
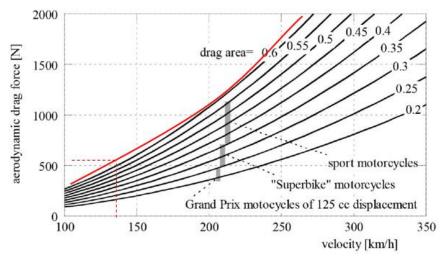

Figure 17. *Graph of velocity, aerodynamic drag force, drag area [19]*

Aerodynamic lift force F_L;

$$F_L = \frac{1}{2}\rho C_L A V^2 \; . \tag{5}$$

Here C_L is the aerodynamic lift coefficient. According to Vittore Cossalter's book [19], $C_LA=0.12$ m^2 is taken. (Upper limit is used.)

It has been determined in the experiments and road tests that the tire rolling resistance F_w corresponds to approximately 2% of the total motorcycle weight [19]. In this way,

$$F_W = \frac{2}{100}mg \; . \tag{6}$$

To find the force of inertia caused by the acceleration of the motorcycle, the values obtained in the "Acceleration Time Test" are used. According to this; As a result of four acceleration tests, the arithmetic average time value found to reach 100 km/h was determined as 17.9 s. (Performance tests were carried out at the beginning of this PhD with the use of a test bike. This article does not contain detailed information about ground tests)

$$\overrightarrow{a_H} = \frac{\Delta\overrightarrow{v}}{\Delta t} \tag{7}$$

$$\overrightarrow{a_H} = \frac{100 \text{ km/h}-0}{17.9 \text{ s}-0} = \frac{27.7 \text{ m/s}}{17.9 \text{ s}}.$$

The acceleration is found to be 1,5 m/s^2.Thus, the inertial force during acceleration is found by the Equation (8)

$$\overrightarrow{F_I} = m.\overrightarrow{a_H} \quad . \tag{8}$$

In line with the assumptions given earlier, a motorcycle in linear motion is taken into account. It is assumed that the motorcycle balance equations written for steady-state motion also apply to vertical translation and rotation. Thus, if Newton's Second Law of Motion is used, horizontal balance of forces in acceleration;

$$-S + F_D + F_W + F_I = 0 \ . \tag{9}$$

Using the results (4), (5), (6) and (8) from Equation (9), the drive force of the motorcycle S is found in the negative direction. Here, assuming that the m.g, S, F_W, F_D, F_L and F_I forces act on the plane of the CoG, for the dynamic load on the front wheel during maximum acceleration (130 km/h), according to Figure 16;

$$-N_f.\,p \ + \ m.\,g.\,b - F_L.\,b - F_D.\,h + S.\,0 - F_W.\,0 - F_I.\,h = 0 \ . \tag{10}$$

N_f is found from Equation (10). Likewise, the rear wheel dynamic load is derived from the moment balance;

$$N_r.\,p - \ m.\,g.\,(p-b) + F_L.\,(p-b) - F_D.\,h + S.\,0 - F_W.\,0 - F_I.\,h = 0 \ . \tag{11}$$

Accordingly, the force values to be applied to the hybrid frame in the acceleration dynamic analysis are given in Table 4.

Table 4. *Force values to be applied in acceleration dynamic analysis*

Forces	Weight, m.g [N]	Front Wheel Load, N_f[N]	Rear Wheel Load, N_r[N]	Lift Force, F_L[N]	Drag Force, F_D[N]	Tire Rolling Resistance, F_W[N]	Inertia Force, F_I[N]	Drive Force, S [N]
Steel frame	-2744.0	692.60	1960.09	91.30	566.8	54.8	420.0	-1041.7
Hybrid frame	-2644.43	663.84	1889.28	91.30	566.8	52.8	404.76	-1026.5

The driving force (S) acting on the frame;

$$M_s = S.\,h \ . \tag{12}$$

M_S moment will be reflected (The sign is negative because it is clockwise relative to the CoG). Tire Rolling Resistance (F_W) acting on the frame;

$$M_{FW} = F_w.\,h \tag{13}$$

M_{FW} moment will be reflected (The sign is positive because it is counterclockwise with respect to the CoG.). The normal force (N_f) on the front wheel is reflected directly to the frame without being damped, despite the wheel and front fork shock absorbers. The force under real use conditions will be much lower than this value. The same is true for the rear wheel force acting on the frame as well.

The application of the boundary conditions to the model is given in Figure 18, two moment values applied are shown in the figure. Moments are applied directly to force the frames.

Figure 18. Application of boundary conditions in acceleration for Hybrid Frame

In this context, after applying a cylindrical support, two displacement supports, seven forces and two moments to the analysis model, the total deformation results for the acceleration analysis are given in Figure19. Equivalent (Von-Misses) Stresses are given in Figure 20.
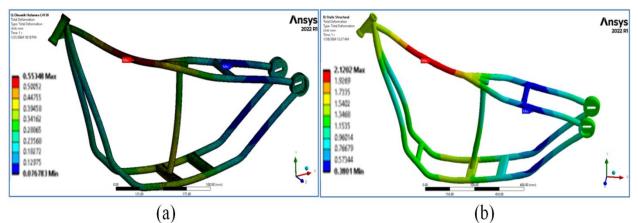

Figure 19. Total deformation for acceleration (a) Steel frame (b) Hybrid frame
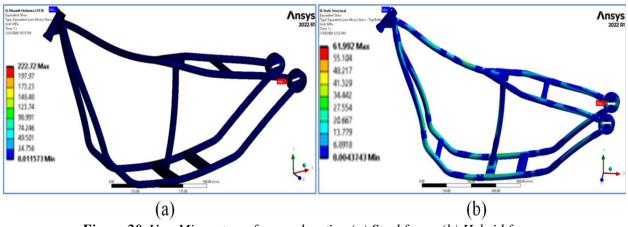

Figure 20. Von-Mises stress for acceleration (a) Steel frame (b) Hybrid frame

After the acceleration load analysis, the region where the maximum stresses occur in the hybrid frame are shown in Figure 21.
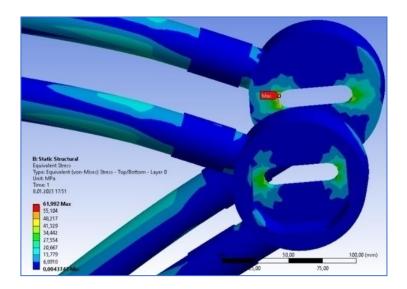
Figure 21. *Region of highest equivalent (Von-Mises) stress in acceleration*

Comparison of acceleration loading analyzes of steel and hybrid frames is shown in Table 5.

Table 5. *Comparison of steel and hybrid frames for acceleration*

Nm.	Feature/Analysis result	Units	Steel frame	Hybrid frame
1	Max. total deformation	[mm]	0.55	2.12
2	Max. equivalent Von-Mises stress	[MPa]	222.72	61.99
3	Safety coefficient	-	2.3	4.0

It is seen that the values of both frames are low in terms of total deformation. Max. deformation occurred in the backbone region of both frames. It is estimated that the values will be lower if the engine and transmission is mounted on the frames.

Equivalent (Von-Misses) Stress value is max. 61.992 MPa. Maximum stress is observed in the rear axle housing part of the frame. According to the analysis results, it was determined that the safety coefficient of the hybrid frame is s=4.04 according to the 251 MPa value, which is the safety stress of the AlSi10 Mg material specified in the Table 2. According to the results of the acceleration analysis, the stress values in the other parts of the frame with CFRP composite tubes and AISI 4130 materials are quite low, the safety coefficients are high, around s=18.0, and the frame provides very high strength.

Comparing the acceleration analysis of the two frames, there is not much difference between the total deformations, but the safety factor of the hybrid frame is about twice that of the steel frame, thus it is seen that the hybrid frame shows more strength.

3.4. Maximum Braking Load Analysis

Driving safety, in addition to an efficient braking system, requires the driver to be able to evaluate the required stopping distance under various conditions, to be able to brake optimally using all the possibilities of the braking system and especially using the rear brake. In fact, many motorcycle riders tend to forget about the rear brake, which is a useful addition in certain situations. Proper use of the rear brake is important both for braking when cornering and for braking during linear movement when an unforeseen obstacle appears in front of the motorcycle.

In this section, all the forces that may affect the frame of the motorcycle during braking while the motorcycle is traveling at 90 km/h will be considered (Figure 22).
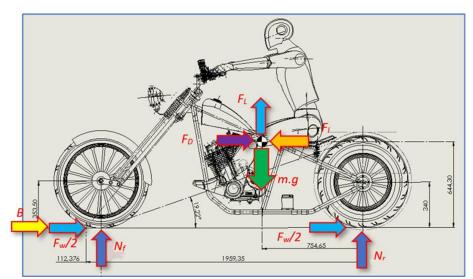
***Figure 22.** Forces acting on the motorcycle during braking for Hybrid Frame*

In the braking calculation, the values of F_L aerodynamic lift, F_D aerodynamic drag and Fw tire rolling resistance forces will be applied with the values when the vehicle is at 90 km/h. In the real case, these forces are gradually reset to zero from the start of braking until the vehicle comes to a stop. However, the highest values will be used in the calculations. This, like the factor of safety, will increase the reliability of the calculations. In addition, B braking force will be calculated according to 90 km/h speed in calculations. In the real situation, when the braking starts, the engine driving force does not affect the motorcycle due to the cut-off of the gas, but the inertial force that occurs at that speed.

To find the inertial force (F_I) resulting from braking; First of all, the deceleration should be detected. In this context, when the equation of motion is applied by assuming the braking efficiency as 100%, the approximate stopping distance [22];

$$\overrightarrow{V_{last}}^2 = \overrightarrow{V_{first}}^2 - 2.\overrightarrow{a_F}.s \; . \tag{14}$$

Here, $\overrightarrow{V_{last}}$ speed after braking, $\overrightarrow{V_{first}}$ starting speed of braking, $\overrightarrow{a_F}$ deceleration, s is the distance traveled during braking. Since the final velocity will be zero at the time of stop, from Equation (14);

$$0^2 = \overrightarrow{V_{first}}^2 + 2.\overrightarrow{a_F}.s$$

$$s = -\frac{\overrightarrow{V_{first}}^2}{2.\overrightarrow{a_F}} \; . \tag{15}$$

To find the inertia force caused by the braking of the motorcycle; Values obtained in the Motorcycle Braking Test will be used. According to this; As a result of the three braking tests, the arithmetic average of the distance values obtained during braking at a speed of 90 km/h (25 m/s) was determined as 26.1 m.

If these values are put in their place in Equation (15), $\overrightarrow{a_F}$ is found. In this framework, the inertial force during braking is found by Equation (16)

$$\overrightarrow{F_I} = m.\overrightarrow{a_F} \; . \tag{16}$$

The drag force F_D acting on the frames is found by Equation (4) and the aerodynamic lift force F_L is found by Equation (5).

The braking force B, which tries to stop the motorcycle at 90 km/h by establishing the balance of horizontal forces in braking, is found from the Equation (17)

$$B + F_D + F_W - F_I = 0 . \tag{17}$$

Here the dynamic load on the front wheel (N_f) during 90 km/h is found from Equation (18) according to Figure 22

$$-N_f. p + m. g. b - F_L. b - F_D. h - B. 0 - F_W. 0 + F_I. h = 0 . \tag{18}$$

Again, the dynamic load on the rear wheel (N_r) during braking from 90 km/h is found from Equation (19) according to Figure 22

$$N_r. p - m. g. (p - b) + F_L. (p - b) - F_D. h - B. 0 - F_W. 0 + F_I. h = 0 . \tag{19}$$

In this framework, the force values to be used in the braking analysis are given in Table 6.

Table 6. *Force values to be applied in braking dynamic analysis*

Forces	Weight, m.g [N]	Front Wheel Load, N_f[N]	Rear Wheel Load, N_r[N]	Lift Force, F_L[N]	Drag Force, F_D[N]	Tire Rolling Resistance, F_W[N]	Inertia Force, F_I[N]	Braking Force, B[N]
Steel frame	-2744.0	2037.5	662.7	43.8	271.7	54.9	−3351.6	3025.0

The M_B moment consisting of braking force and the M_{FW} moment consisting of tire rolling resistance were calculated. Boundary conditions applied in the ANSYS program are shown in Figure 23.
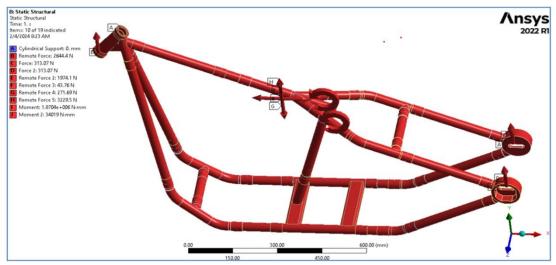

Figure 23. *Boundary conditions for frame dynamic load analysis in braking for Hybrid Frame*

After applying a cylindrical support, two displacement supports, seven forces and two moments to the analysis model, the total deformation results for the braking analysis are given in Figure 24. Also, Equivalent (Von-Misses) Stresses are given in Figure 25, and Comparison of braking loading analyzes of steel and hybrid frames is shown in Table 7.
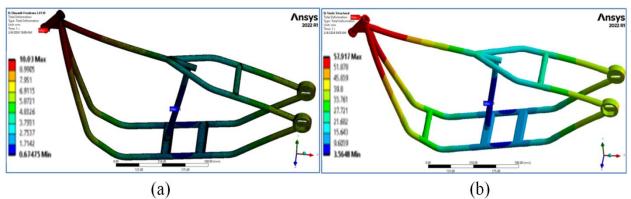
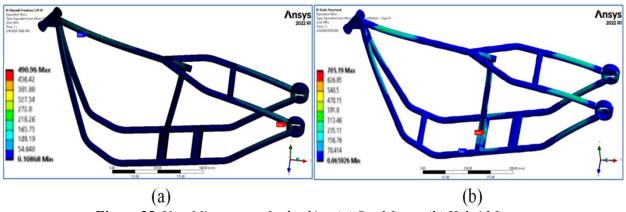**Figure 24.** *Total deformation for braking (a) Steel frame (b) Hybrid frame*

Figure 25. *Von-Mises stress for braking (a) Steel frame (b) Hybrid frame*

Table 7. *Comparison of steel and hybrid frames for braking*

Nm.	Feature/Analysis result	Units	Steel frame	Hybrid frame
1	Max. total deformation	[mm]	10.03	57.91
2	Max. equivalent Von-Mises stress	[MPa]	490.96	705.19
3	Safety coefficient	-	1.03	0.72

In terms of max. total deformation, it is seen that the deformation value of the hybrid frame (57.9 mm) is considerably higher than the deformation value of the steel frame (10.0 mm). It is considered that the deformations in the neck of the frame will be much lower under real operating conditions due to the presence of springer fork and front wheel.

As can be seen in Figure 25 (b), maximum stress occurred only on the bottom of the seat tube which is made of AISI4130 steel. According to the analysis result, it has been determined that the safety coefficient of the hybrid frame is s=0.72, according to the 507.8 MPa safety stress specified in Table 2. Although the strength values in other parts of the hybrid frame are observed to be quite high according to the color map of Ansys, it is seen that the stress at the bottom of the seat tube exceeds the strength limits. In fact, it is considered that the strength problem can be eliminated by applying two or three passes of the weld at the junction of the tube and profile, but it would still be appropriate to go for a more radical design improvement. Improvement work will be given at the end of the study.

In the braking situation, the steel frame seems to be more durable than the hybrid frame under current conditions.

3.5. Effect of Centrifugal Force on Frame (Cornering Load Analysis)

When the motorcycle is in steady rotation, it is subject to both a restoring moment created by the centrifugal force, which tends to rotate the motorcycle to a vertical position, and a tipping moment and roll angle created by the weight force, which tends to increase.

Considering a motorcycle while cornering in a stationary state; The balance of moments of forces acting on the CoG shows that the normalized lateral force required to stabilize the motorcycle is equal to the tangent of the roll angle (φ) as shown in Figure 26 [19].
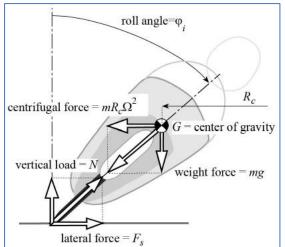

Figure 26. *Cornering stability, steady turning and rolling angle of a motorcycle equipped with zero-thickness tires [19]*

In this study, strength calculations will be made by assuming that the lateral force F_S, which is caused by the turning of the motorcycle in the corner, can be reliably covered by the motorcycle tire. As indicated in Figure 26, the motorcycle tire thickness was taken into consideration as zero. In this framework, camber thrust, rolling angle and lateral slip relations, which vary according to motorcycle tire characteristics, are not taken into account.

Centrifugal force (N) is calculated by Equation (20);

$$F_C = m.R_c.\omega^2 \quad . \tag{20}$$

Here R_c turning radius (m), ω or Ω angular velocity (Hz, 1/s), m is mass of object (kg).

If only the angular velocity ω is known, it can be recalculated in terms of normal velocity by multiplying it by the circumference of the circular path. If the following equation is used;

$$v = \omega.R_c \quad . \tag{21}$$

Here v is linear velocity (m/s). If Equation (21) is substituted in Equation (20);

$$F_C = m.\frac{v^2}{R_c} \quad . \tag{22}$$

The relationship between centrifugal force and linear velocity of the vehicle is shown in Figure 27.
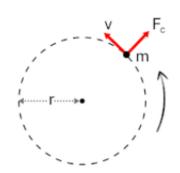
Figure 27. *Relationship between centrifugal force and linear velocity [23]*

Since the motorcycle entering the bend at a maximum speed of 130 km/h does not meet the safety requirements, the speed of entering the bend is accepted as 60 km/h (16.6 m/s) as a safe speed, and the radius of the turn is taken as 50 m.

The drag force F_D acting on the frames is found by Equation (4) and the aerodynamic lift force F_L is found by Equation (5). The tire rolling resistance F_w is found by Equation (6).

As a result of four acceleration tests, the arithmetic average time value found to reach 100 km/h was determined as 17.9 s. With the proportional method, the time to reach 60 km/h is 10.7 seconds.

The acceleration $\overrightarrow{a_H}$ is found by Equation (7), the inertia force $\overrightarrow{F_I}$ is found by Equation (8). The forces acting on the motorcycle while cornering are given in Figures 16 and 26.

Centrifugal force (Fc) is at the CoG and inward from the picture plane and lateral force (Fs) is outward from the picture plane at the point where the front and rear wheels touch the ground.

In this context, if Newton's Second Law of Motion is used, the motorcycle driving force S is found from Equation (9) according to the balance of vertical forces in the x-y plane at the bend.

Taking the rolling angle as φ=45°, N_f is found by Equation (23) according to Figure 16 for the dynamic load on the front wheel during 60 km/h speed

$$-N_f.\,p \;+\; m.\,g.\,b - F_D.\,(h.\cos45) + S.\,0 - F_W.\,0 - F_I.\,(h.\cos45) - F_L.\,b = 0. \tag{23}$$

Equation (24) is used to find N_r with the same method

$$N_r.\,p - \; m.\,g.\,(p-b) - F_D.\,(h.\cos45) + S.\,0 - F_W.\,0 - F_I.\,(h.\cos45) + F_L.\,(p-b) = 0\;. \tag{24}$$

The forces to be used in the analysis of the motorcycle turning in the corner are given in Table 8.

Table 8. *Force values to be applied in cornering dynamic analysis*

Forces	Weight, m.g [N]	Front Wheel Load, N_f[N]	Rear Wheel Load, N_r[N]	Lift Force, F_L[N]	Drag Force, F_D[N]	Tire Rolling Resistance, F_W[N]	Inertia Force, F_I[N]	Acceler. Force, S [N]
Steel frame	-2744.0	917.59	1807.11	19.29	119.78	54.88	420.0	-594.66
Hybrid frame	-2644.43	886.49	1738.25	19.29	119.78	52.88	415.49	-588.15

In the corner, the lateral force F_S is found according to the Equation (25) deduced from the balance of horizontal forces in the y-z plane

$$F_s - F_c = 0 \quad . \tag{25}$$

The calculated lateral force (F_S) will be reflected in the frame as the M_{FS} moment in the yz plane. The direction sign is negative according to the right-hand rule

$$M_{FS} = F_s. h. \cos45 \quad . \tag{26}$$

The Tire Rolling Resistance (F_W) will be reflected to the frame as the M_{FW} moment. The direction sign is positive according to the right-hand rule

$$M_{FW} = F_w. h. \cos45 \quad . \tag{27}$$

The acceleration force (S) will be reflected to the frame as the M_S moment. The direction sign is negative according to the right-hand rule

$$M_S = S. h. \cos45 \quad . \tag{28}$$

In this context, the forces and moments acting on the frames are shown in Figure 28. The total deformation results for the cornering analysis are given in Figure 29. Also, equivalent (Von-Misses) Stresses are given in Figure 30.

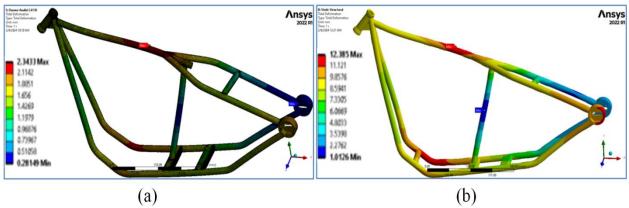**Figure 28.** *Boundary conditions for frame dynamic load analysis in cornering for Hybrid Frame*

(a)   (b)

Figure 29. *Total deformation for cornering (a) Steel frame (b) Hybrid frame*
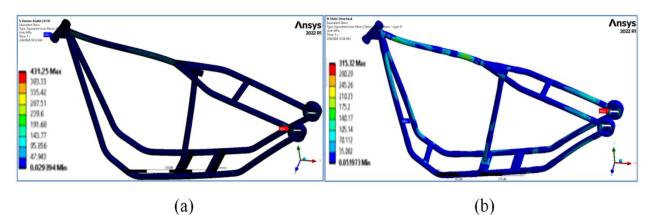
Figure 30. *Von-Mises stress for cornering (a) Steel frame (b) Hybrid frame*

Comparison of acceleration loading analyzes of steel and hybrid frames is shown in Table 9. In terms of max. total deformation, it is seen that the deformation value of the hybrid frame (12.38 mm) is considerably higher than the deformation value of the steel frame (2.34 mm). It is considered that the maximum deformations in the backbone region of the frame will be much lower under real operating conditions due to the engine and transmission integration.

Table 9. *Comparison of steel and hybrid frames according to the analysis results*

Nm.	Feature/Analysis result	Units	Steel frame	Hybrid frame
1	Max. total deformation	[mm]	2.34	12.38
2	Max. equivalent Von-Mises stress	[MPa]	431.25	315.32
3	Safety coefficient	-	1.2	0.8

The region of maximum stress in the cornering analysis of the hybrid frame is shown in Figure 31. The maximum stress in a very small part of the frame including the rear axle housing bore edges are detailed in Figure 31. The safety limit has been exceeded only in the region where the AlSi10Mg 3D printing material is located. Since there is no alternative material other than this material during the production phase, 3D printed parts (AlSi10Mg) will be used in the production of prototype frame, and the condition of the frame will be observed by performing crack control tests with the penetrant liquid method periodically. In the following period, it is evaluated that the problem of exceeding the safety limit can be eliminated by using a more durable material with the material development situation in 3D printing technology. In addition, since the loads on the frame are applied directly during the analysis, it is considered that the intensity of the loads on the frame will decrease with the help of the rear wheels under normal operating conditions. An exaggerated representation of the deformation of the hybrid frame according to the forces and moments it is subjected to in the cornering analysis is given in Figure 32.
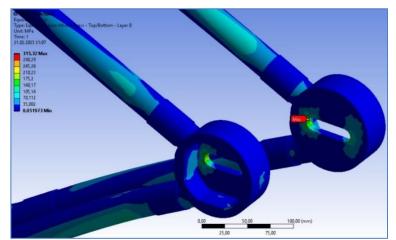

Figure 31. *The region of max. stress in the cornering analysis of the hybrid frame*
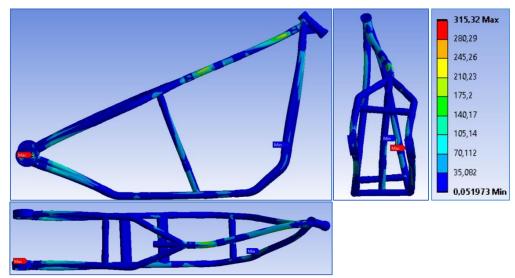
Figure 32. *An exaggerated representation of the deformation of the hybrid frame in cornering*

In addition, it can be said that the hybrid frame has high strength in the other parts containing CFRP and steel material according to the Ansys color mapping, except for the AlSi10Mg rear axle housings where the maximum stress is detected.

4. DESIGN IMPROVEMENT

It was decided that it would be appropriate to make a design improvement, especially for the stress exceeding the strength limits determined at the bottom of the seat tube as a result of the braking analysis. In this context, an additional rectangular profile and a gusset were placed in the stress region, as seen in Figure 33.

After the parts were added to the design, the equivalent stress (von mises) result after the new braking analysis performed under the same boundary conditions is given in Figure 34.

As can be seen in Figure 34, after the design intervention, the safety factor of 0.72 for the hybrid frame (Table 7) was increased to 1.2 and it was pulled into the strength limits.
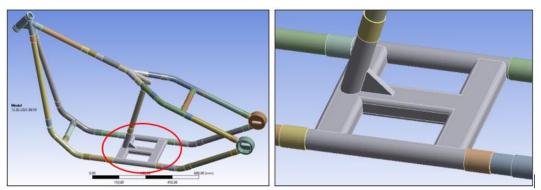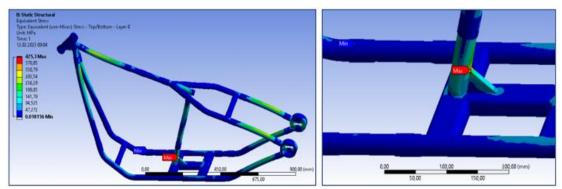

Figure 33. *The design improvement of the hybrid frame*

Figure 34. *The equivalent stress (Von-Mises) result of the hybrid frame*

5. RESULTS

In this study, strength analyses were performed under static and dynamic loads for a prototype study trial of a chopper-type motorcycle frame using the finite element method. For this purpose, a lighter hybrid frame structure consisting of a combination of various materials (steel, CFRP and aluminum) was designed and the results obtained were compared with a steel frame. A total of four different analyses, including static, acceleration, braking and cornering, were applied to the frame, whose weight was reduced by 10.16 kg with the targeted material change. When all analyses are taken into account, it has been observed that the total deformation values of the steel frame are lower than the hybrid frame. The fact that the tube joints of the steel frame are made by welded manufacturing ensures that the steel frame has a more rigid structure. The joints of the hybrid frame were joined by the bonding method, and it had more joints than the steel frame. For this reason, the deformation values are considered to be high. In addition, no weakness was detected in terms of strength at the joints of the hybrid frame combined with epoxy resin in any analysis. It is expected that the total deformations will be much lower under real operating conditions by mounting the springer fork, engine-transmission group, shock absorbers and wheels on the motorcycle frame. In terms of equivalent stress analysis, it is seen that the stress and safety coefficient values of the hybrid frame are almost two times better than the steel frame in the case of static and acceleration loading. As for the braking and cornering analysis, it is seen that the strength values of the steel frame are better than the hybrid frame. In addition, it is seen that the parts of the hybrid frame containing AlSi10Mg and AISI 4130 materials exceed the strength limits, while the parts containing CFRP material show high strength properties.

It is evaluated that the maximum total deformation values of the Hybrid Chassis are generally higher than those of the Steel Chassis, the reason for this is that the Hybrid Chassis has a more jointed structure than the Steel Chassis due to its design and the rigidity of the Steel Chassis is higher than that of the Hybrid Chassis due to the fact that the parts are joined by welded manufacturing, and that the deformation values that occur under real usage conditions will be much lower than those obtained in the analyses since the engine-transmission, fuel tank and hydraulic shock absorber front fork are mounted on the chassis.
It is thought that the areas where maximum deformation occurs in the Steel Chassis are generally the weld joints, and that in case of steel chassis production, the strength of these areas can be improved by applying 2-3 rows of weld seams to the joint areas.

While the use of motorcycles has become widespread all over the world due to the savings it provides to the user in time and fuel with the increased courier services after the Covid-19 epidemic, the number of motorcycles registered in Turkiye reached 5 million 5 thousand 666 in the period of January-November 2023 [24]. In the literature and industrial sector researches, it is seen that there are many bicycle frames produced using composite materials, but there are limited number of chassis production studies including composite materials for motorcycles, and the existing studies are mostly aimed at monoblock (body consisting of a single piece) frame productions. With this study, a chassis consisting of multi-piece material combination is produced by integrating carbon fiber pipes cut to appropriate dimensions into aluminum and steel joint parts produced by additive manufacturing, which has not been seen before in the literature and industrial sector, and by using the same engine-transmission group in this chassis, it is aimed to reduce

weight, increase current speed and reduce fuel consumption compared to another chassis containing only steel pipes in the same dimensions.

When considered in terms of production style, quite high mold costs will occur for the production of a composite monoblock chassis and these molds will need to be re-manufactured for each design/size change. In this study, it is evaluated that the hybrid chassis created by integrating ready-made CFRP tubes with aluminum and steel joining parts will have lower production costs, design and dimensional changes can be compensated more easily by changing the tube lengths compared to a monoblock chassis, and the ability to change regional features can be gained by using tubes made of different materials in the chassis in general and/or sections. A monoblock motorcycle chassis made of composite material is shown in Figure 35a, and a motorcycle chassis made of tubes (tubular) is shown in Figure 35b.

(a)   (b)

***Figure 35.** (a) Monoblock and (b) Tubular Motorcycle Chassis*

In addition, in the acceptances made for the hybrid chassis, it was evaluated that the parts produced by additive manufacturing had the properties of a cast material and the analyses were carried out according to this point of view. It is thought that it would be very useful to conduct project studies focusing on the effects of parts produced by additive manufacturing on similar strength analyses in the future.

On the other hand, it is considered important to expand the scope of the analyses applied in this study and to perform analysis studies by adding the engine-transmission and other subsystems to the finite element analysis in order to obtain more realistic results.

As a result, in an article published in Motorsport Magazine, one of the respected magazines of the motorcycle world, on February 07, 2024; It was stated that sooner or later every racer competing in MotoGP will have a carbon fiber frame, because in addition to being light, carbon fiber frames provide much better road grip. Again, in the same article, it is emphasized that motorcycle frames with "situational awareness" capability, which allows the frame to perceive instantaneous situations, can be produced through the use of electrically conductive plastic fibers in a composite structure [25].

ACKNOWLEDGMENT

CONFLICTS OF INTEREST

No conflict of interest was declared by the authors.

ABBREVIATIONS AND SYMBOLS

SYMBOL	MEANING of SYMBOL
CFRP	Carbon Fiber Reinforced Polymer
FEM	Finite Element Method
F_w	Tire Rolling Resistance Force
F_D	Aerodynamic Resistance Force to Forward Motion
F_L	Lifting Force
F_I	Inertia Force
F_C	Centrifugal Force
S	Driving Force of the Motorcycle Engine
ρ	Material Density
A	Area
C_D	Aerodynamic Resistance (Drag) Coefficient
V	Motorcycle Forward Speed
C_L	Aerodynamic Lift Coefficient
COG	Center of Gravity
N_{sf}	Motorcycle Front Wheel Load
N_{sr}	Motorcycle Rear Wheel Load
$\vec{a}_H$	Acceleration
$\vec{a}_F$	Deceleration
s	Safety Factor
M_s	Moment of Driving Force S
M_{FW}	Moment of Tire Rolling Resistance Force F_w
B	Breaking Force
R_c	Turning Radius
Ω, ω	Angular Velocity

REFERENCES

[1] Mateusz, A., Arkadiusz, D., Piotr, S., "Motorcycle chassis design: frame development for the PreMoto3 motorcycle", 10th International Conference on Research in Science and Technology, 18-20 December, Oxford, UK, 55-67, (2020).

[2] Fentahun, M.A., Savaş, M.A., "Materials Used in Automotive Manufacture and Material Selection Using Ashby Charts", International Journal of Materials Engineering, 8(3): 40-54, (2018).

[3] Jeyapandiarajan, P., Kalaiarassan, G., Joel, J., Shirbhate, R., Telare, F.F., Bhagat, A., "Design and analysis of chassis for an electric motorcycle", Materials Today: Proceedings, 5(5): 13563-13573, (2018).

[4] Dama, K.K., Malyala, S.K., Babu, V.S., Rao, R.N., Shaik, I.J., "Development of automotive flexbody chassis structure in conceptual design phase using additive manufacturing", Materials Today: Proceedings, 4(9): 9919-9923, (2017).

[5] Mat, M.H, Ghani, A.R. Ab., "Design and analysis of 'eco' car chassis", Procedia Engineering, 41:1756-1760, (2012).

[6] Rechena, D., "Motorcycle frame analysis", IDMEC/IST, Master Thesis, Institute of Mechanical Engineering, Instituto Superior Técnico, University of Lisbon, Portugal, (2014).

[7]   Liang, Z., Cheng, L., Kiet, T., "Fatigue analysis of a motorcycle frame system based on a road test and the finite element method", Materials Science Forum, 773-774:842-850, (2014).

[8]   Tripathi, S., Ambikesh, R.K., "Design and FEA of motorcycle frame using carbon/flax hybrid composite as a light weight substitute to steel", International Research Journal of Engineering and Technology (IRJET), 8(6): 4554-4557, (2001).

[9]   Neeraja, C.H., Sireesha, C.R., Jawaharlal, D., "Structural analysis of two wheeler suspension frame", International Journal of Engineering Research & Technology (IJERT), 1(6): 1-6, (2012).

[10]   Slaiman, H., "Strength and stiffness analysis of motorcycle frame", Master's Final Degree Project, Kaunas University of Technology, Faculty of Mechanical Engineering and Design, Kaunas, Lithuania, (2018).

[11]   Information on https://www.motorcyclistonline.com/carbon-fiber-technology-carbon-framed-future-for-bmw. Access Date: 22.12.2015

[12]   Information on https://www.motorsportmagazine.com/articles/motorcycles /motogp/carbon-fibre-motogp-it-s-long-story. Access Date: 02.09.2019

[13]   Garofano A, Acanfora V, Fittipaldi F, Riccio A. "On the use of a hybrid metallic-composite design to increase mechanical performance of an automotive chassis", Journal of Materials Engineering and Performance, 32(9): 3853-3870, (2023).

[14]   Foale, T., "Motorcycle handling and frame design-The art and science", (2002).

[15]   Iso 5751-1, Motorcycle tires and rims-Part 1: Design guides.

[16]   Iso 5751-2, Motorcycle tires and rims (Metric Series)-Tyre sizes and Load carrying capacities.

[17]   Iso 4249-3, Motorcycle tires and rims- Part 3: Rims.

[18]   Information on https://chopperbuildershandbook.com. Access date: 14.04.2020

[19]   Ansys (Version 2019 R2), Finite Element Analysis (FEA) Software, https://www.ansys.com/. Access date: 01.01.2019

[20]   Kanani, A.Y., "Ansys Tutorial for Acp (Full composite tutorial in Ansys)", University of Kent, UK, (2017).

[21]   Cossalter, V., "Motorcycle Dynamics", Gardners Books Limited Eastbourne, (2006).

[22]   Bayrakceken, H., Duzgun, M., "Brake efficiency and braking distance analysis in vehicles", Journal of Polytechnic, 8(2):153-160, (2005).

[23]   Information on https://learnool.com/centrifugal-force-equation, Access date: 14.10.2023

[24]   Number of Motorcycles in Traffic Exceeded 5 Million for the First Time, Anadolu Agency (Web page). Access date: May 2024

[25]   KTM tech: 'sooner or later everyone will have carbon-fibre frames', https://www.motorsportmagazine.com/ (Web page) Access Date: 07.02.2024